

Influence of an ultrasonic field on lead electrodeposition on copper using a fluoroboric bath

Elena Agulló, José González-García, Eduardo Expósito, Vicente Montiel* and Antonio Aldaz

Departamento de Química Física, Universidad de Alicante, Apartado 99, 03080 Alicante, Spain;
E-mail: vicente.montiel@ua.es

Received (in Montpellier, France) 22nd June 1998, Revised m/s received 18th September 1998, Accepted 19th October 1998

The influence of three different types of stirring: mechanical, ultrasonic and a combination of both, on the mass transport coefficient and on the characteristics of the deposit of lead on copper electrodes has been studied. The results obtained show that ultrasounds always provide higher mass transport rates than mechanical stirring. The best deposition characteristics are obtained at 35 °C using a combination of ultrasound and mechanical stirring. Normally, ultrasounds increase the quality of the deposit by decreasing the number and size of dendrites. However, the sonication time has a strong influence on the adherence of the deposits. Thus, for long sonication times, part of the lead deposit detaches itself from the surface, giving deposits of very poor quality. A preliminary study of lead deposition on three-dimensional copper foam electrodes was made and similar results were obtained. With mechanical stirring, the interior of the foam was not coated with lead while when combined stirring was used, better results were obtained. However, for long sonication times the mechanical stability of copper foams is strongly decreased and the electrode is destroyed.

A 3D lead electrode, obtained by deposition of lead on a carbon felt, has been used for the synthesis of L-homocysteine from L-homocystine in which a current density—relative to the projected area of the electrode—of 500 mA cm⁻² has been employed.¹ However, these type of electrodes do not have very good mechanical characteristics and can develop a high contact resistance between the feeder current plate and the felt. Moreover, to obtain a uniform deposit of lead on this type of electrode is not easy and the electrode has a hydrogen overpotential that is not as high as it would be if all the carbon surface were covered by lead. Lead foams would be better but they are not commercially available in large dimensions and they are also too soft to be used in an electrochemical cell. Thus, a good solution would be a copper felt or foam electrode covered by lead, in which better electric contact can be made by soldering the foam to the feeder plate. Moreover, this type of electrode is more mechanically stable than the carbon felt electrode. Copper foams can be obtained in large dimensions and the construction of big electrodes is possible. The final objective of our research is to obtain lead deposits on copper foams to be used as high hydrogen overvoltage electrodes. However, deposition of lead on the inside of the foam failed when using lead solutions stirred in the customary way by mechanical methods.

One way to increase the stirring of a solution is by application of an ultrasonic field. During the propagation of ultrasonic waves in the liquid, secondary effects such as cavitation, acoustic flows and acoustic pressure appear. These effects cause intensive turbulent flows throughout the liquid and near the interface, which considerably diminishes the diffusion layer thickness.² Another reason for using an ultrasonic field in electrodeposition in aqueous solution is that acoustic vibrations affect three other important factors: (1) the physical and chemical properties of the solution, by accelerating redox reactions and decreasing the gas content in the liquid, as well as other effects;³ (2) the metallic electrode surface, by removing impurities and dirt from pipes and microfissures from the metallic surface^{3,4} and (3) the nucleation processes (or the cre-

ation of a crystallization centre) and the growth of crystals.^{4,5} The use of ultrasounds permits the electrodeposition of metals with higher current densities than those normally used without reducing efficiency and the deposit microstructure is also improved.

Because ultrasounds cause an increase in the stirring of the solution, a preliminary study was necessary in which the first objective was the quantification of the mass transport produced by ultrasounds and its comparison with mechanical stirring. The second part of this work was to study the influence of ultrasounds and temperature on the characteristics of the lead deposits. But, taking into consideration the difficulties that can appear by using electrodes with complex geometry, it was decided to begin with an initial study of the influence of ultrasounds using planar electrodes. To sum up, the aim of this work (prior to obtaining three-dimensional deposits) is to carry out a comparative study of the influence of three different types of stirring, by ultrasound, mechanically and by a combination of both methods, on the rate of mass transport to planar electrodes and on the influence of these stirring types on the morphology (adhesion and edge effects) of the lead deposits. Moreover, preliminary experiments on lead deposition on foam copper electrodes will be presented and discussed.

Experimental

The experimental setup employed for obtaining the electrochemical deposits, and for which the mass transport was characterized, is shown in Fig. 1(a). The ultrasonic field is produced by an ultrasonic cleaning bath (Ultrasons 3000513 from Selecta) that has a frequency of 30 kHz and 150 W power consumption (92 W of transmitted power measured with the calorimetric method by placing the thermometer probe at 5 cm from the transducer, in a position central with respect to it). The solution can be mechanically stirred by recirculating the solution with a pump (flow: 100 L h⁻¹,

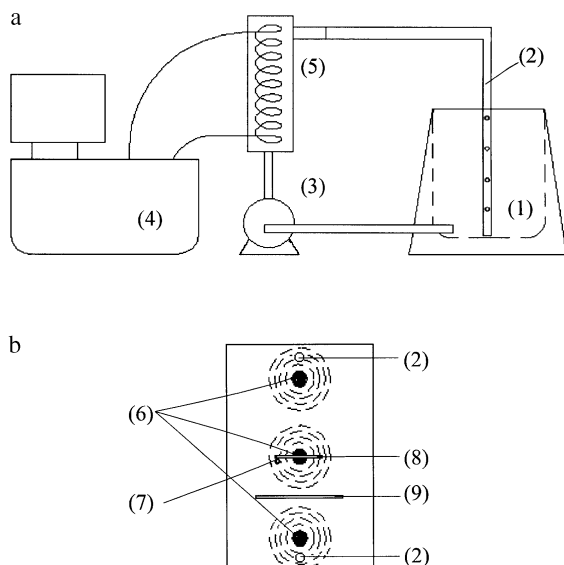


Fig. 1 (a) Diagram of the experimental equipment and (b) upper view of the position of the electrodes in the ultrasonic bath. (1) Ultrasonic cleaning bath, (2) recirculating outlet tube, (3) pump, (4) constant temperature bath, (5) heat exchanger, (6) transducers, (7) the luggin capillary of the reference electrode, (8) cathode and (9) anode.

residence time: 216 s). The stirring types studied and characterized are: (1) ultrasonic stirring (US), when only ultrasounds are active in the bath; (2) mechanical stirring (M), when only recirculation of the solution takes place and (3) combined stirring (US + M), when the ultrasound field and the recirculation of the solution operate simultaneously.

The selected temperatures were 25, 35, 46 and 55 °C. In order to maintain the temperature constant during the experiments with mechanical and combined stirring, the solution was passed through a heat exchanger [(5) in Fig. 1], in contact with a thermostating bath [(4) in Fig. 1] in which the temperature was constant. A digital thermometer was placed into the solution (Crison 638) and the variation of the temperature was within $\pm 0.5^\circ\text{C}$. During the characterization of mass transport with ultrasonic stirring the following procedure was followed: the solution reached the desired temperature by recirculation, using the experimental setup of Fig. 1. Just before carrying out the experiment the recirculation circuit was disconnected and the transient was recorded under ultrasounds. As the measurement took less than 1.5 min, the temperature variation was acceptable, within $\pm 1^\circ\text{C}$ for 46 and 55 °C and $\pm 2^\circ\text{C}$ for 25 and 35 °C. During deposition with ultrasonic stirring the temperature was controlled by two glass cooling coils inserted in the solution, through which water was circulated from a constant temperature bath (temperature variation $\pm 0.5^\circ\text{C}$).

As a model system for the measurement of the mass transport coefficients, the Cu(II) reduction to metallic copper was used. The solution [$0.71\text{ g L}^{-1}\text{ Na}_2\text{SO}_4$, H_2SO_4 up to pH = 2 and between 0 and $0.12\text{ g L}^{-1}\text{ CuSO}_4 \cdot 5\text{H}_2\text{O}$ as Cu(II) source] is similar to that used in other work⁶ and references therein. As the working electrode, a smooth sheet of copper was used. In order to maintain the copper concentration in the bath constant, a copper anode was employed. The area of the cathode varied from 1.08 to 1.19 cm², according to the experiment, and the dimension of the counter electrode was always 16 cm². The distance between the electrodes was 4 cm and the distance from the cathode to the ultrasound transducer was 3 cm. The position of the cathode was central with respect to the transducer, as can be seen in Fig. 1(b). The bath was a closed bath in which the oxygen was removed by N₂ bubbling. Nitrogen was also used to saturate the solution with gas before each experiment. Thus, we ensured that the cavi-

tation threshold in the experiments did not change since it depends on the number of bubbles that exist in the solution and that act as cavitation nuclei.⁷

In order to determine the limiting current, I_L , the potential step method was used. A step from -50 to -500 mV (*vs.* saturated calomel electrode, SCE) placed the system at a potential where the reaction was mass transport controlled.⁶ Current-time curves were recorded for each concentration, stirring type and temperature. The instruments used were an Amel potentiostat, model 2055, an EG&G Parc signal generator, model 175, and an X/t-Y Kipp&Zonen recorder.

Lead electrodeposition was carried out at constant current electrolysis using a Blausonic 30 V 2.5 A power supply. A coulometer ESC 640 was employed to measure the charge. The cathode was a copper plate whose area varied from 5.0 to 6.0 cm² (the change in the cathode area between the k_m and electrodeposition experiments was simply to perform the adhesion test under better conditions). We have to emphasize that the trend of k_m with temperature gives us an idea of the type of stirring that provides a bigger mass transport for every temperature and thus, k_m values have to be regarded as indicative. In order to maintain the lead concentration constant during the deposition and for plating the cathode on both sides, two perforated lead anodes of 36 cm² were employed. The electrode gap was 4 cm.

The influence of the three types of stirring, as well as temperature and current density on the characteristics of the lead deposit was also studied. The selected temperatures were 35 and 55 °C and the current density varied between 10 and 200 mA cm⁻². The electrodeposition solution was: 42 g L⁻¹ of HBF₄, 30 g L⁻¹ of H₃BO₃, 0.2 g L⁻¹ of peptone and 50 g L⁻¹ of Pb(II) as PbO.⁸ The surface treatment applied to the copper plates was the same for all the experiments and consisted of the chemical removal of the copper oxide layer by attacking it with HNO₃ (1 : 1, for 5 min), followed by abrasion with sand (particle diameter between 100 and 150 μm, 5 psi pressure, for 3 min) to ensure a good adhesion.⁹ The distance between the cathode and the ultrasound transducer was maintained at 5 cm. (Preliminary results with the cathode at 1, 3 and 5 cm from the transducer showed that 5 cm was the best distance, instead of 3 cm, which was the distance during the k_m determination.) The position of the electrode was central relative to the transducer [Fig. 1(b)].

In order to study the homogeneity, porosity and dendritic formation in the lead deposit, scanning electron microscopy (SEM) was employed. The surface composition was determined by using electron dispersion spectroscopy (EDS or X-ray analysis). Adhesion was measured by the adhesive band technique.¹⁰ The scanning electron microscope used was a Jeol JSM-840 and the X-ray analyser was a Link X-Ray Analytical System QX200.

Results and discussion

Mass transport coefficient measurements with the copper system

In order to characterize the mass transport in a given system, the mass transport coefficient, k_m , is employed. This coefficient is a heterogeneous velocity constant that together with the electroactive concentration characterizes the rate of mass transport. This coefficient changes with temperature and flow conditions.¹¹ To determine k_m , the limiting current expression for mass transport controlled reactions is used:

$$I_L = nFAk_m c \quad (1)$$

where n is the number of transferred electrons, F is the Faraday constant, A is the electrode area and c is the electroactive species concentration.

The current transients obtained with the potential step technique are shown in Fig. 2 and 3 for 35 and 55 °C, respectively.

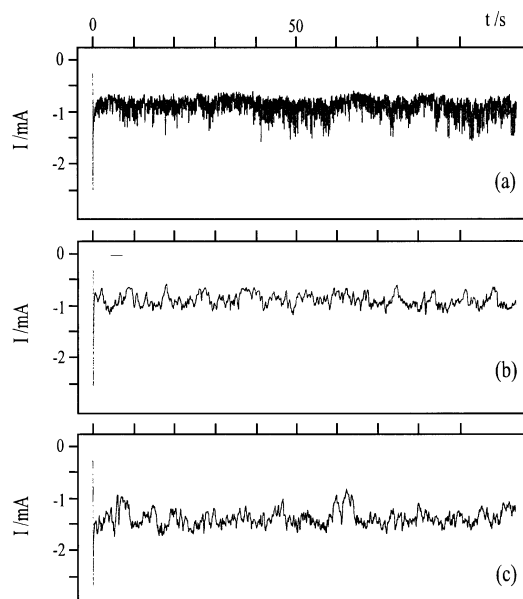


Fig. 2 Current transients for a $0.71 \text{ g L}^{-1} \text{ Na}_2\text{SO}_4$, $\text{pH} = 2$, $[\text{Cu(II)}] = 0.06 \text{ g L}^{-1}$ solution at $T = 35^\circ\text{C}$. Potentiostatic steps from -50 to -500 mV (vs. SCE). (a) US, (b) M and (c) US + M stirring.

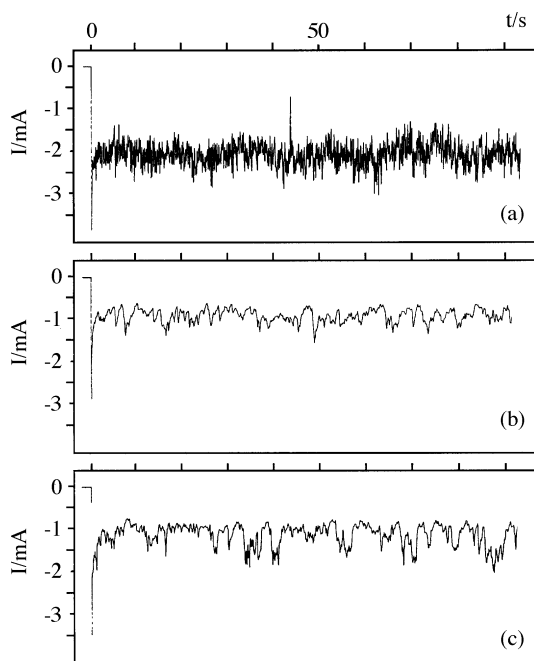


Fig. 3 Current transients for a $0.71 \text{ g L}^{-1} \text{ Na}_2\text{SO}_4$, $\text{pH} = 2$, $[\text{Cu(II)}] = 0.06 \text{ g L}^{-1}$ solution at $T = 55^\circ\text{C}$. Potentiostatic steps from -50 to -500 mV (vs. SCE). (a) US, (b) M and (c) US + M stirring.

For each temperature and copper concentration, three curves were recorded, one for each stirring type.

The transients obtained with ultrasounds are characterized by high amplitude fluctuations, in accordance with the oscillatory behaviour of ultrasounds [Fig. 2(a) and 3(a)]. The current profile shows the presence of pulses as a result of the collapse of the cavitation bubbles, which takes place at the electrode surface. The different amplitudes of the pulses can be interpreted by the existence of different distances of these collapsing bubbles to the electrode since the maximum radius of the cavitation bubbles is approximately the same for all the collapsing bubbles.¹² In our case, because the electrode has a large area, the different amplitudes also depend on the number of bubbles that collapse simultaneously on the surface electrode. The current clearly reaches a constant value. According to Hagan and Coury¹³ and to Compton *et al.*,¹⁴ the limiting current is composed of a spatially averaged value or steady current (which they called dc current) and a transient portion (ac current), whose sum gives the instantaneous value of the current. However, the current fluctuations are expected to average to a constant value if a large enough electroactive surface is employed. This is the case for the size of electrodes employed here. Furthermore, Compton *et al.* demonstrated¹⁴ that the ac component of the current followed a linear correlation with the area of the electrodes when macroelectrodes were used.

The current transients, Fig. 2(b) and 3(b), obtained with mechanical stirring clearly show the non-homogeneous mass transport caused by this type of stirring.

With regard to the shape of the combined stirring curves, Fig. 2(c) and 3(c), it can be seen that these do not have the characteristic fluctuations of acoustic vibrations (US). On the contrary, their shape is very similar to that obtained with mechanical stirring, curves (M), and do not change appreciably with temperature, although at low temperatures the suppression of the effect caused by ultrasounds is less marked. These results clearly point out that mechanical stirring masks some of the effects of ultrasounds.

The values of I_L are obtained as the average value of the current transients and are given in Table 1. These I_L values, plotted vs. copper concentration, gave straight lines whose slopes allow us to calculate k_m [eqn. (1)]. An example is shown in Fig. 4 for a temperature of 55°C . The k_m values obtained for different temperatures and stirring types are shown in Table 2. The data show that ultrasonic irradiation considerably increases mass transport at 46 and 55°C . However, for 25 and 35°C , the highest values of k_m correspond to those obtained with combined stirring. Thus, in any case, the presence of the ultrasonic field increases the mass transport of the electroactive species from the bulk of the solution to the electrode surface.

As far as the temperature influence is concerned, k_m for both mechanical and ultrasonic stirring increases as temperature rises. In the absence of an ultrasound field, (M), k_m

Table 1 Limiting current density values obtained at 25 , 35 , 46 and 55°C for ultrasonic (US), mechanical (M) and combined (US + M) stirring

$[\text{Cu(II)}]/\text{g L}^{-1}$	$j_L/\text{mA cm}^{-2}$											
	25°C			35°C			46°C			55°C		
	US	M	US+M	US	M	US+M	US	M	US+M	US	M	US+M
0.00	0.00	0.00	0.00	0.00	0.00	0.00	0.00	0.00	0.00	0.00	0.00	0.00
0.02	0.10	0.12	0.25	0.15	0.15	0.26	0.39	0.18	0.33	0.47	0.19	0.22
0.04	0.21	0.23	0.45	0.47	0.30	0.55	0.79	0.37	0.66	0.82	0.39	0.48
0.06	0.34	0.34	0.70	0.56	0.48	0.77	1.27	0.56	1.08	1.35	0.64	0.78
0.08	0.46	0.48	0.89	0.91	0.63	0.99	1.74	0.75	1.41	1.98	0.91	1.11
0.10	0.59	0.61	1.18	0.89	0.79	1.23	2.21	0.97	1.76	2.59	1.14	1.43
0.12	0.71	0.76	1.41	1.62	0.99	1.68	2.67	1.19	2.16	3.15	1.39	1.84

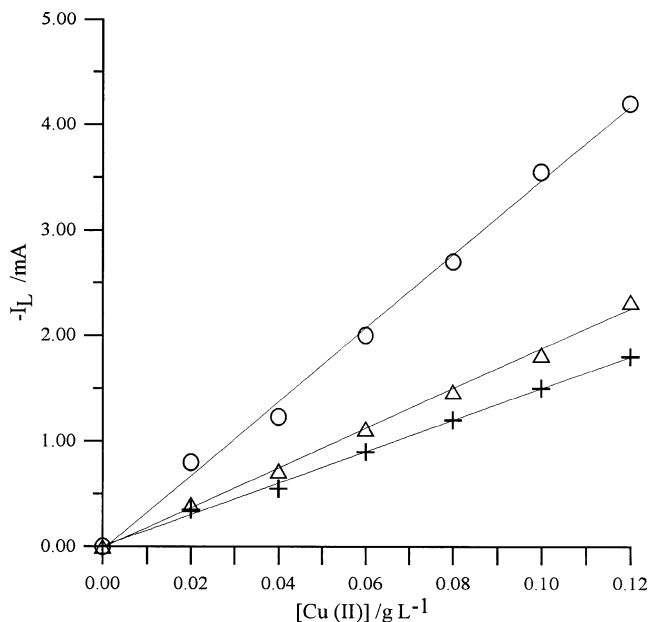


Fig. 4 Limiting current vs. Cu(II) concentration at 55 °C and with (○) US, (+) M and (Δ) US + M stirring.

increases with temperature mainly due to the decrease of the kinematic viscosity of the solution and the increase of the diffusion coefficient of the species transported. However, the intensity of the cavitation collapse caused by ultrasounds is inversely proportional to temperature due to the fact that, at high temperatures, bubbles are filled with more vapour, thus providing a cushion during collapse.¹² It is possible that this effect partially compensates the expected increment in I_L during sonication in the 45–55 °C interval.

With regard to combined stirring, this does not follow the same trend with temperature as ultrasonic stirring. In spite of the fact that k_m for US increases with temperature, k_m for US + M decreases from 45 to 55 °C. It appears that mechanical stirring modifies in some way the effect of the ultrasounds. A possible explanation for this phenomenon is that the solution that flows in one direction, due to the mass flow caused by mechanical stirring, debilitates the oscillatory component in the opposite direction induced by acoustic vibration, in a similar way to what happens with mechanical vibrations.¹⁵ This is also in agreement with what is shown in Fig. 2 and 3, where the shapes of the transient curves for US + M and for M are similar.

Lead electrodeposition on smooth copper electrodes under sonication

At this point, we are only interested in the homogeneity of the deposit, that is with little or no dendritic growth. One simple way of relating the influence of ultrasounds on the deposit is by what we have defined as the “deposition

Table 2 Mass transport coefficient values obtained at 25, 35, 46 and 55 °C for ultrasonic (US), mechanical (M) and combined (US+M) stirring

$T/^\circ\text{C}$	$k_m \times 10^5/\text{m s}^{-1}$		
	US	M	US+M
25	2.1	2.1	3.9
35	4.0	2.7	4.4
46	7.4	3.3	6.0
55	8.8	3.9	5.1

efficiency”, DE. This is the ratio between the charge consumed to deposit the lead that remains adhered to the support and the total charge circulated, expressed as a percentage. This efficiency can be calculated from the change in the electrode weight before and after the electrodeposition process. The deposition efficiency calculated in this way is the same as the current efficiency of the process only when all the lead deposited remains on the support.

Fig. 5 and 6 show the influence on the deposition efficiency of the different types of stirring for different current densities at 55 and 35 °C, respectively, and for a total charge passed of 79.2 C cm^{-2} , which was the same for all the experiments. In Fig. 6 the results of mechanical stirring were not considered because of the bad adherence of the obtained deposits.

In the absence of ultrasounds, (M), the curve shows the behaviour that could be normally expected: the deposition

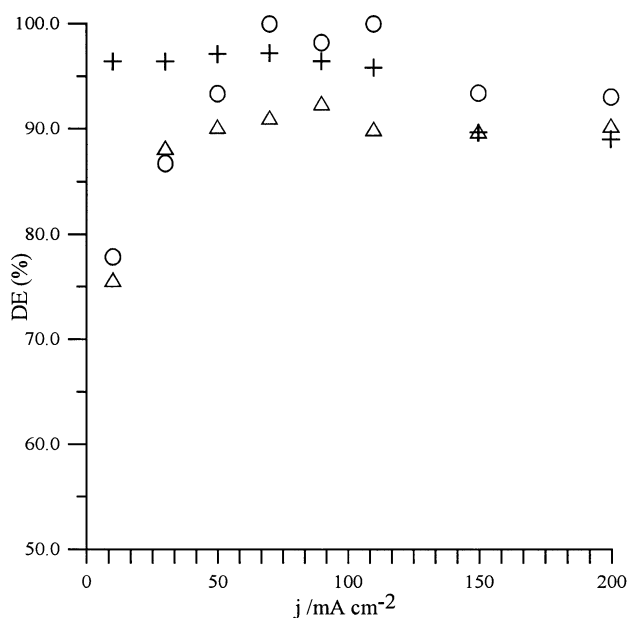


Fig. 5 Deposition efficiency vs. current density at 55 °C and with (○) US, (+) M and (Δ) US + M stirring.

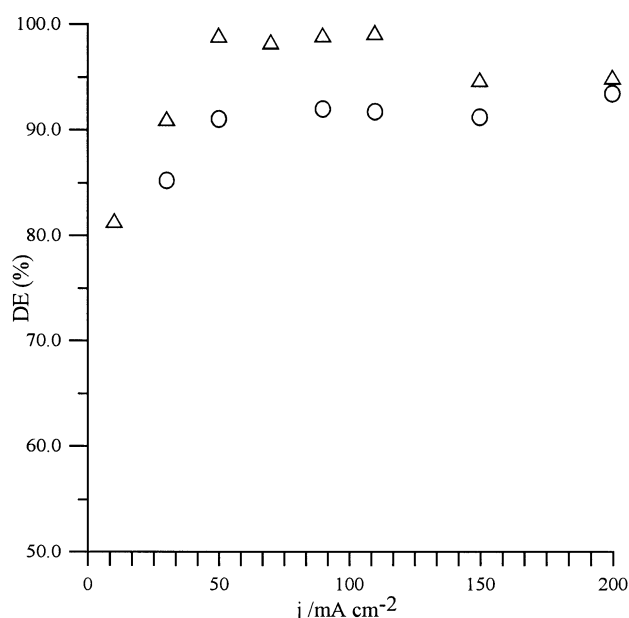


Fig. 6 Deposition efficiency vs. current density at 35 °C and with (○) US and (Δ) US + M stirring.

efficiency remains constant at low current densities and diminishes for high current densities. In this case, deposition efficiency is approximately the same as current efficiency because the deposit did not flake off and remained adhered to the electrode (only the dendrites formed on the border are detached). For ultrasonic and combined stirrings, the curves vary in a similar way, the deposition efficiency goes through a maximum. This behaviour is abnormal because the current efficiency is at a maximum for lower current densities and decreases as the current density increases.

At low current densities, flakes of lead appear in the solution. The explanation for this behaviour is that sonication causes the lead deposit to fall away proportional to the sonication time. Thus, taking into account that the deposit is carried out at constant charge, the sonication time will be longer as the current density decreases and in this way increase the loss of the deposit. Fig. 7(a) and (b) correspond to the deposits obtained for current densities of 10 and 50 mA cm⁻², that is, for different sonication times, and clearly show that an increase in the sonication time causes a loss of the lead deposit and that for low currents the deposit is more granulated and less homogeneous.

At intermediate current densities, the deposition efficiency remains constant and is at its highest value. At high current densities, the deposition efficiency diminishes once again. This time it is due to a decrease of the current efficiency because hydrogen evolution appears and no lead flakes are found in the solution.

Dendritic formation on the border of the electrodes, the edge effect, strongly decreases with sonication. The dimensions and quantity of dendrites decrease when deposits are made in an ultrasonic field. Fig. 8 shows photographs of the deposits on the edge of the electrodes for the different types of stirring. These deposits were obtained at 55 °C and 90 mA cm⁻². The difference is even greater when the deposition is carried out at low current densities for which dendrites do not form at all when using ultrasonic stirring.

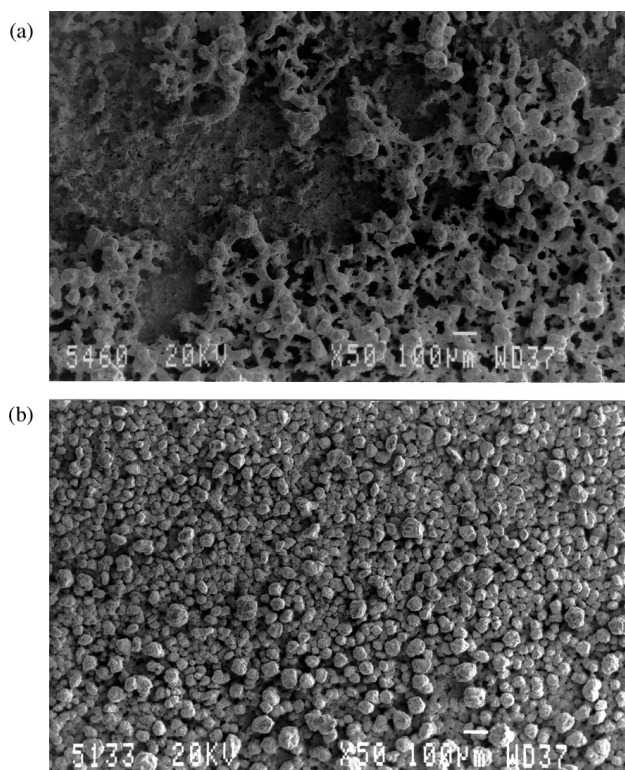


Fig. 7 SEM micrographs of lead deposits obtained at 35 °C with US + M stirring. Current densities of (a) 10 mA cm⁻² and (b) 50 mA cm⁻².

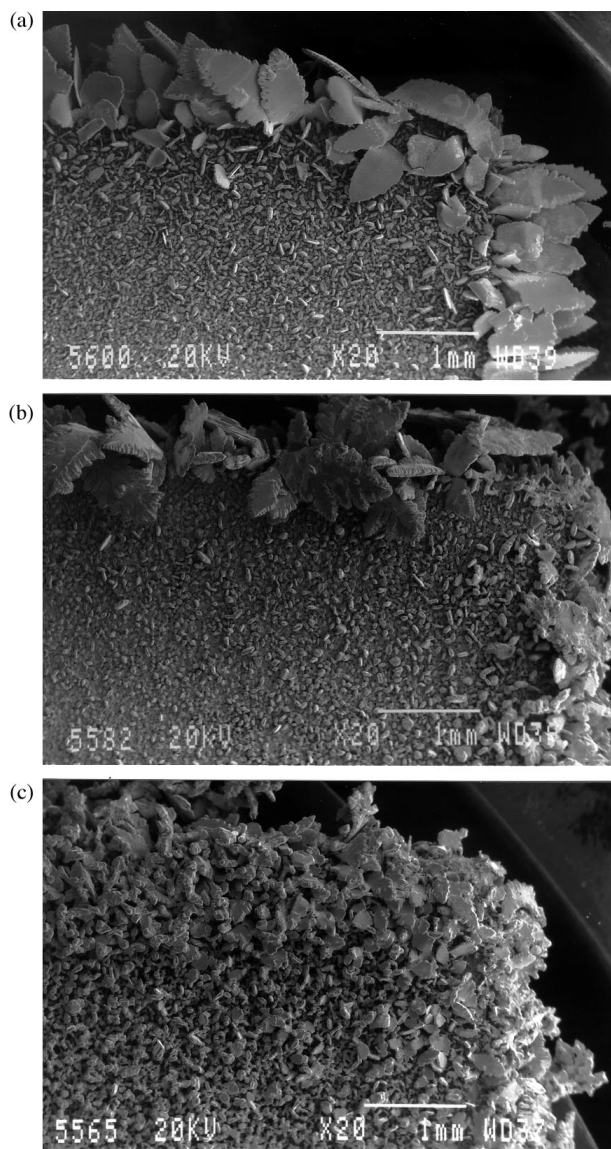


Fig. 8 SEM micrographs of lead deposits obtained at 55 °C and 90 mA cm⁻² with (a) M, (b) US + M and (c) US stirring.

Finally, some depositions were performed under the same electrodeposition conditions but in varying the cathode-to-transducer distance. This variation changes the power of the ultrasounds on the electrode surface. The distances studied were 1 and 5 cm. In Fig. 9, in which deposition efficiency is plotted *vs.* current density, it can be seen that efficiencies were better when the electrode was placed 5 cm from the ultrasound source than when it was only 1 cm from it. The reason is clearly shown by comparing Fig. 10 with Fig. 7(b). The grain size increases when the distance is 1 cm and at the same time a large part of the substrate is free of lead. For this distance, lead flakes are present in the solution. The deposit obtained at a distance of 5 cm is more homogeneous, with smaller grain size and without flakes. It is obvious that proximity to the ultrasound source is harmful to the deposits (so the influence of the power of the ultrasonic field on the characteristics of the lead deposits must be very important).

With regard to the quality of the deposits, the best conditions for lead electrodeposition on copper seem to correspond to 35 °C and combined stirring. Under these conditions, the deposits had good adherence, good deposition efficiency and negligible dendritic growth. Despite the fact that at 55 °C and with US the mass transport velocity was the highest and that the deposits were obtained without dendrites, the adhesion was not so good as that obtained for 35 °C and US + M.

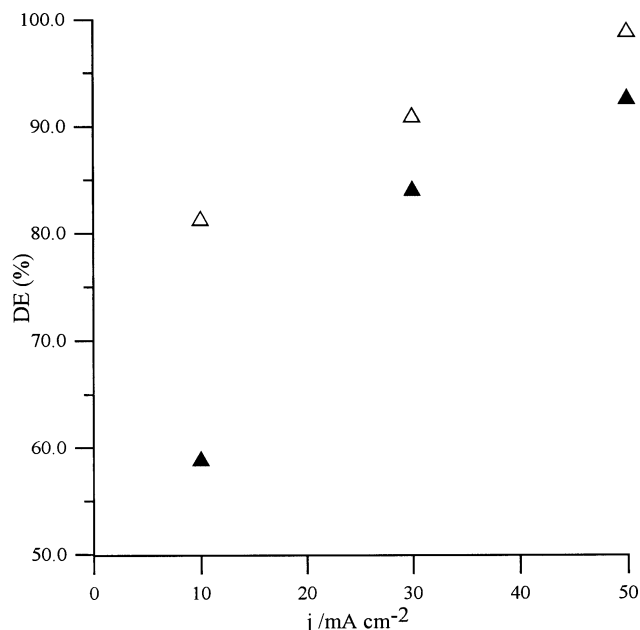


Fig. 9 Deposition efficiency vs. current density at 35 °C and US + M stirring. Cathode-to-transducer distances: (▲) 1 and (△) 5 cm.

Lead electrodeposition on copper foam electrodes under sonication

The decrease of dendritic growth is of great importance when three-dimensional lead electrodes are to be obtained by depositing lead on copper foams. The complex geometry of the substrate leads to a poor and non-uniform mass transport that causes the formation of dendrites in most of its volume, producing plated electrodes of very bad quality. For developing 3D lead electrodes we have used the results and experience obtained during the study of lead deposition on smooth copper electrodes. Thus, a preliminary study of lead deposition on copper foams has been carried out at 35 °C using the same experimental conditions and solution employed in the former study. Fig. 11 shows the results obtained for the three different stirring types at 10 mA cm⁻². It is clearly seen that with mechanical stirring the deposit does not cover the total surface of the electrode because the inner part of the copper foam is not coated at all, while for the combined stirring lead covers most of the interior of the foam. As with two-dimensional electrodes, the deposition efficiency is poor at this current density. However, when employing different values of the current density only the use of combined stirring permits good deposits in foams to be obtained. It must be pointed out that the use of ultrasounds only causes

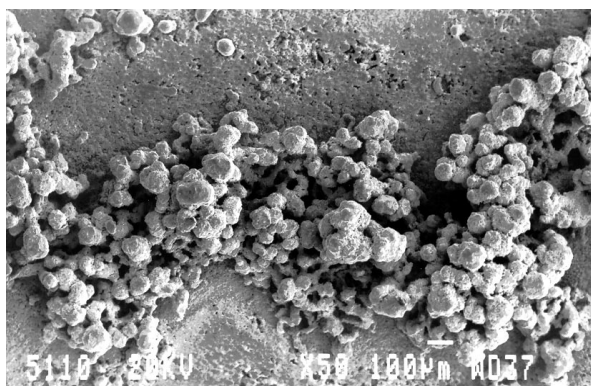


Fig. 10 SEM micrograph of a lead deposit obtained at 35 °C with US + M stirring, 50 mA cm⁻² and a cathode-to-transducer distance of 1 cm.

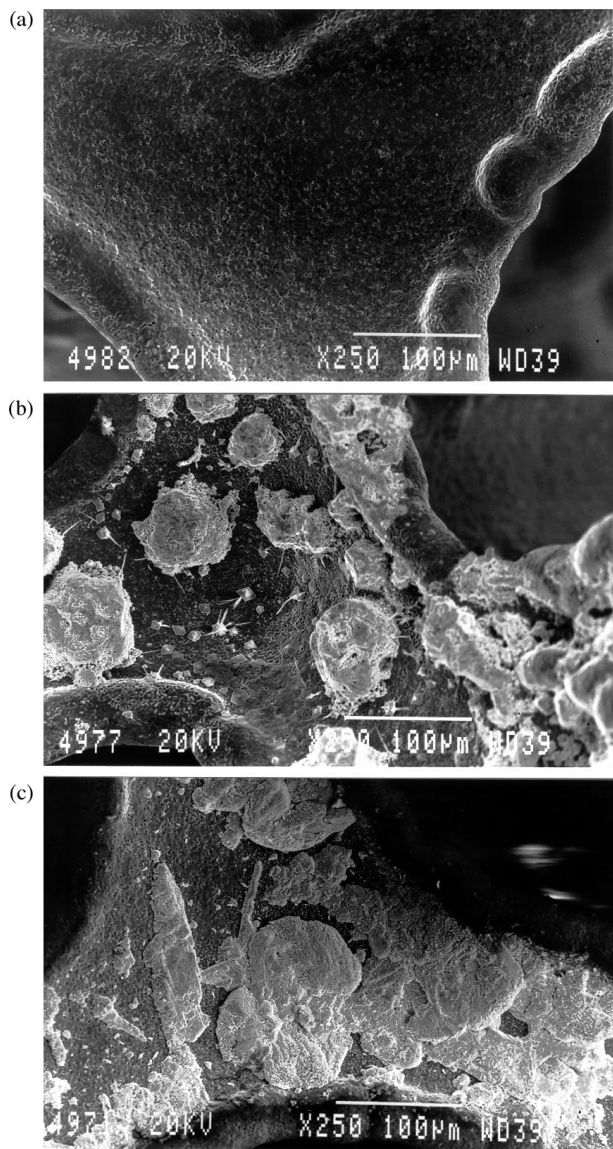


Fig. 11 SEM micrographs of lead deposits, on the interior of copper foams, obtained at 35 °C and 10 mA cm⁻² with (a) M, (b) US, and (c) US + M stirring.

physical damage to the copper foam, partially destroying the electrode. This means that the ultrasound power must play an important role in the characteristics of the deposit on these 3D electrodes. More work is in progress to try to optimize and characterize lead deposits on copper foam electrodes by using an electrochemical reactor in which the power and frequency of the ultrasounds can be varied.

Conclusions

In the interval of temperature studied, cavitation collapse increases with temperature until it reaches a maximum. This makes the mass transport coefficient dependence on temperature (both with mechanical stirring, US + M, and without it, US) more complex than when ultrasounds do not exist. The dependence was as follows: at 35 °C and lower temperatures, the highest values of k_m correspond to combined stirring. At temperatures higher than 35 °C, the highest k_m corresponds to ultrasonic stirring. Furthermore, it was found that the deposition efficiency of lead on copper follows the same tendency as the mass transport coefficient with temperature and stirring, which was to be expected since at higher mass transport rates, a larger quantity of electroactive species reaches the electrode

and then the deposition efficiency increases at even higher current densities, unusual in an electrodeposition process.

With regard to electrodeposition, it was found that as the electrodeposition time in ultrasounds decreases, the deposition efficiency and the properties of the deposits improve. The edge effect is also strongly influenced by the presence of an ultrasonic field and the formation of dendrites diminishes when electrodeposition is carried out under ultrasounds. The influence is more noteworthy for lower current densities. Finally, the proximity of the electrode to the transducer during electrodeposition is harmful to deposits, producing flakes and granulated areas with bad adherence and therefore a decrease in the deposition efficiency.

Deposit quality does not follow the same trend as k_m . In the presence of ultrasounds, it appears to be more influenced by the temperature. The best characteristics are achieved at an intermediate temperature (35 °C) and a higher rate of mass transport (US + M).

Acknowledgements

The authors wish to thank Professor José Miguel Martín-Martínez for his help during the adhesion measurements. We also thank CICYT (project QUI97-1086) for financial support.

References

- 1 G. Sánchez-Cano, V. Montiel, V. García, A. Aldaz and E. Elías, in *Electrochemical Engineering and Energy*, ed. F. Lapique, A. Storck and A. A. Wragg, Plenum Press, New York, 1995, p. 151.
- 2 (a) D. J. Walton and S. D. Phull, in *Advances in Sonochemistry*, ed. T. J. Mason, JAI Press, 1996, vol. 4, p. 205; (b) R. G. Compton, J. C. Eklund and F. Marken, *Electroanalysis*, 1997, **7**, 509; (c) A. Benahcene, C. Petrier and G. Reverdy, *New J. Chem.*, 1995, **19**, 989; (d) J. Reisse, H. Francois, J. Vandercammen, O. Fabre, A. Kirsch-de-Mesmaeker, C. Maerschalk and J. P. Delplancke, *Electrochim. Acta*, 1994, **39**, 37.
- 3 A. T. Vagramian and Z. A. Soloviera, in *Le Dépôt Électrolytique des Métaux*, Dunod, Paris, 1958, p. 211.
- 4 B. Agranat, M. Dubrovin, N. Javski and G. Eskin, in *Fundamentos de la Física y la Química de los Ultrasonidos*, Mir, Moscow, 1990.
- 5 J. González-García, J. Iniesta, A. Aldaz and V. Montiel, *New J. Chem.*, 1998, **22**, 343.
- 6 D. Pletcher, in *Electrochemistry for a Cleaner Environment*, ed. D. Genders and N. Weinberg, Electrosynthesis Company Inc., New York, 1992, p. 11.
- 7 L. Broeckaert, T. Caulier, O. Fabre, C. Maerschalk, J. Reisse, J. Vandercammen, D. H. Yang, T. Lepoint and F. Mullie, in *Current Trends in Sonochemistry*, ed. G. J. Price, Royal Society of Chemistry, Cambridge, UK, 1992, p. 8.
- 8 R. Fratesi, G. Roventi, M. Maja and N. Penazzi, *J. Appl. Electrochem.*, 1994, **14**, 505.
- 9 (a) D. Pletcher and F. C. Walsh, in *Industrial Electrochemistry*, Chapman and Hall, London, 1990; (b) D. R. Gabe, in *Principles of Metal Surface Treatment and Protection*, Pergamon Press Ltd, Oxford, 1972; (c) G. Isserlis, in *Industrial Electrochemical Processes*, ed. A. T. Kuhn, Elsevier, Amsterdam, 1971.
- 10 A. J. Kinloch, in *Adhesion and Adhesives*, Chapman and Hall, London, 1987.
- 11 (a) E. Heitz and G. Kreysa, in *Principles of Electrochemical Engineering*, VCH, Weinheim, 1986; (b) F. C. Walsh, in *A First Course of Electrochemical Engineering*, The Electrochemical Consultancy, Romsey, 1993.
- 12 J. Klíma, C. Bernard and C. Degrand, *J. Electroanal. Chem.*, 1994, **367**, 297.
- 13 C. R. S. Hagan and L. A. Coury, *Anal. Chem.*, 1994, **66**, 399.
- 14 R. G. Compton, J. C. Eklund, S. D. Page, T. J. Mason and D. J. Walton, *J. Appl. Electrochem.*, 1996, **26**, 775.
- 15 G. H. Sedahmed, M. Z. El-Abd, A. A. Zatout, Y. A. El-Taweel and M. M. Zaki, *J. Electrochem. Soc.*, 1994, **141**, 437.

Paper 8/04745F